Supplementary Information (SI) for Chemical Communications.

Supporting Information

Modulation in Electronic Structure of Bimetallic FeRu Alloy Nanoparticles for Efficient Alkaline Hydrogen Evolution

Cheng Ye[a], Yu Liu[b], Huamei Tong[b], Mengyue Qi[b], Yong Chen[c], Di Li[a,*] and Deli Jiang[b,*]

[a] Institute for Energy Research, Jiangsu University, Zhenjiang 212013, China

[b] School of Chemistry and Chemical Engineering, Jiangsu University, Zhenjiang 212013, China

[c] Jiangsu SOPO (Group) Co., Ltd, Zhenjiang, Jiangsu 212000, PR China

Corresponding author: Di Li, Deli Jiang

E-mail address: cfbgdd@sina.com, dlj@ujs.edu.cn

Experimental Sections

Materials

Ferric trichloride ($FeCl_3$), potassium hydroxide (KOH), ethylene glycol ($(CH_2OH)_2$), acetone, and absolute ethanol were procured from Sinopharm Chemical Reagent Co., Ltd (Shanghai, China). Platinum/carbon (Pt/C, 20 wt%), ruthenium chloride hydrate ($RuCl_3 \cdot 3H_2O$), Nafion solution (5 wt%) and nickel foam (NF) were bought from Aladdin (Shanghai, China) and Jia Shide Foam Metal Co., Ltd (Suzhou, China). The reagents were utilized directly without any additional treatment, and deionized water was used throughout the experiment.

Treatment of NF

The NF was immersed in 3 mol L^{-1} HCl for 15 minutes. The oxides were then removed from the surface via sonication. Subsequently, the NF was sequentially sonicated in solutions of DI water, ethanol, and acetone, each for 15 minutes. Finally, the NF was then subjected to a drying process in a vacuum.

Preparation of FeRu alloy nanoparticles electrocatalyst

Firstly, the mixture comprised 60 mg $RuCl_3$ and 30 mg $FeCl_3$ was prepared by dissolving each compound in 15 mL of DI water and 15 mL of ethylene glycol, respectively. The mixture was stirred for 30 minutes. Subsequently, the solution was moved to a sealed autoclave lined with Teflon, and the treated NF (2 cm × 5 cm) was placed in a vertical position. The reaction was carried out for 16 hours at 180 °C. Then, the sample was then carefully washed several times at room temperature, followed by vacuum drying at 60 °C for 12 hours. The resultant sample was denoted as Fe_1Ru_2/NF.

The preparation methods of Fe/NF and Ru/NF were similar to that of Fe_1Ru_2/NF. For Fe/NF, $RuCl_3$ was not added during the preparation process, while for Ru/NF, $FeCl_3$ was not added.

Structure Characterizations

The microstructural analysis was conducted using scanning electron scanning electron microscopy (SEM, S-4800 II FESEM), transmission electron microscopy (TEM, FEI JEM-2100), and high-resolution TEM (HRTEM, FEI Tecnai G2 F20). The composition of all catalysts was characterized by an X-ray diffractometer (Bruker D8 Advance X, Cu-Kα radiation, λ = 1.5406 Å, 10°-80°). An ECSA PHI500 spectrometer was used to perform X-ray photoelectron spectroscopy to examine the chemical state of the catalysts' surface.

Electrochemical Measurements

The CHI-760E electrochemical workstation was used to investigate the electrochemical properties in a three-electrode system. The measurements were performed in 1 M KOH aqueous electrolyte, where nickel foam cathode served as working electrodes, graphite as the counter electrode, and Hg/HgO as the reference electrode. The measured potential can be converted to that of a reversible hydrogen electrode (RHE) using the following equation: $E_{RHE} = E_{Hg/HgO} + 0.098\ V + 0.059 \times pH$. Linear sweep voltammetry (LSV) was conducted at a scan rate of 5 mV s^{-1}. Electrochemical impedance spectroscopy (EIS) measurements were carried out over a frequency range of 0.1 to 100 kHz. To evaluate long-term stability, the electrocatalyst was subjected to 5,000 CV cycles at 10 mV s^{-1}. An electric current of 100 mA cm^{-2} was used to evaluate the Faradaic efficiency of the catalyst.

The in situ Raman spectroscopy was conducted using the Zolix Nano/RTS2-301-SMS instrument, employing a laser from Beijing Honglan Photoelectric Technology Co., Ltd. (VCL-488nm M0-30mW), emitting at 532 nm with a power of 10 mW. The signal was recorded with a 10 s integration time, scanned four times, and accumulated accordingly. The in situ electrochemical three-electrode cell contained a Fe_1Ru_2 electrocatalyst as the working electrode, Hg/HgO as the reference electrode and graphite as the counter electrode. The electrolyte used was 1.0 M KOH, and the measured potential for the HER was in the range -1.00 ~ -1.55 V.

Computational Methodology

DFT calculations were carried out using the Vienna Ab initio Simulation Package (VASP) with the projector-augmented plane-wave (PAW) to describe the core electrons.[1,2] The Perdew–Burke–Ernzerhof (PBE) functional within the generalized gradient approximation (GGA) was adopted for the exchange–correlation term.[3] For the plane-wave basis set, the cutoff energy was fixed at 450 eV, and the convergence criterion of self-consistent total energy was less than 1×10^{-5} eV while the residual forces on each atom of structural optimization was set to converge within a threshold of 0.02 eV $Å^{-1}$. The long-range van der Waals interactions were corrected by using Becke-Jonson damping DFT-D3 method. The Ru (100), Fe (100) and Fe_1Ru_2 (100) planes were built as the crystal models, and all of these models were structure optimized.

The E_{ads} were calculated using the equation:

$$E_{\mathrm{ads}} = E_{\mathrm{ad/sub}} - E_{\mathrm{ad}} - E_{\mathrm{sub}}$$

where the $E_{ad/sub}$, E_{ad}, and E_{sub} are the total energies of the adsorbate/substrate system, the adsorbate in the structure, and the clean substrate, respectively.[4,5]

The adsorption energy change (ΔG_{H*}) was calculated from Equation (1)

$$\Delta G_{H*} = \Delta E_{H*} + \Delta E_{ZPE} - T\Delta S_{H} \quad (1)$$

Where ΔE_{H*}, ΔE_{ZPE}, T, and ΔS_{H} represent the hydrogen chemisorption energy change, zero-point energy change, temperature and entropy change, respectively.[6–8]

References

1 G. Kresse, J. Furthmüller, *Comp. Mater. Sci.*, 1996, **6**, 15.

2 P. E. Blöchl, *Phys. Rev. B*, 1994, **50**, 17953.

3 J. P. Perdew, J. A. Chevary, S. H. Vosko, K. A. Jackson, M. R. Pederson, D. J. Singh, C. Fiolhais, *Phys. Rev. B*, 1992, **46**, 6671.

4 J. Yang, T. Xie, Y. Mei, J. Chen, H. Sun, S. Feng, Y. Zhang, Y. Zhao, J. Wang, X. Li, J. He and H. Chen, *Appl. Catal. B-Environ.*, 2023, **339**, 123149.

5 Y. Liao, J. Qian, G. Xie, Q. Han, W. Dang, Y. Wang, L. Lv, S. Zhao, L. Luo, W. Zhang, H.-Y. Jiang and J. Tang, *Appl. Catal. B-Environ.*, 2020, **273**, 119054.

6 S. Grimme, J. Antony, S. Ehrlich, H. Krieg, J. Chem. Phys., 2010, **132**, 154104.

7 H. Liang, H. Zou, S. Hu, *New J. Chem.*, 2017, **41**, 8920.

8 F. Du, L. Shi, Y. Zhang, T. Li, J. Wang, G. Wen, A. Alsaedi, T. Hayat, Y. Zhou, Z. Zou, *Appl. Catal. B-Environ.*, 2019, **253**, 246.

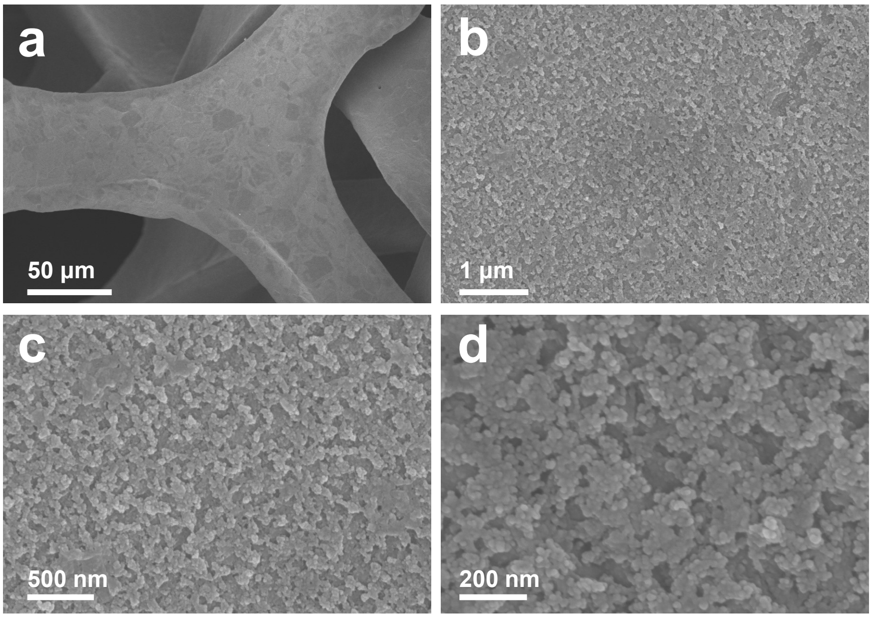

Fig. S1 SEM images of Fe_1Ru_2/NF.

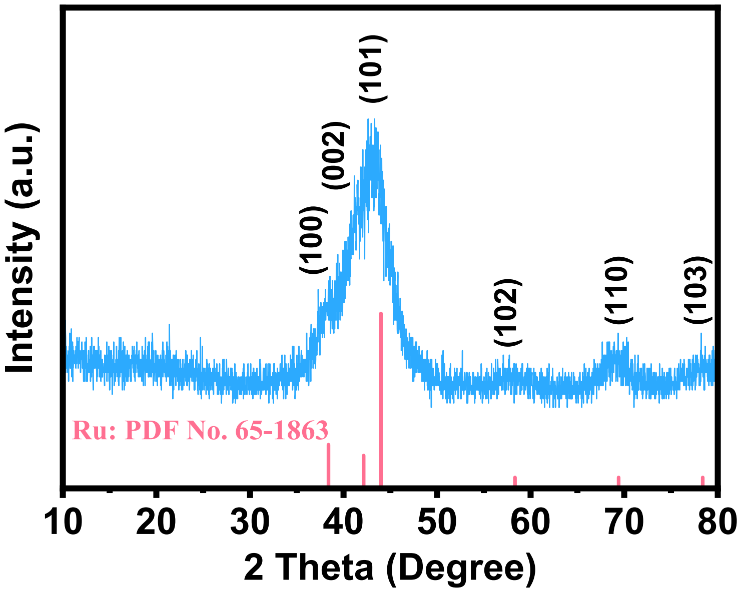

Fig. S2 XRD pattern of the Ru/NF.

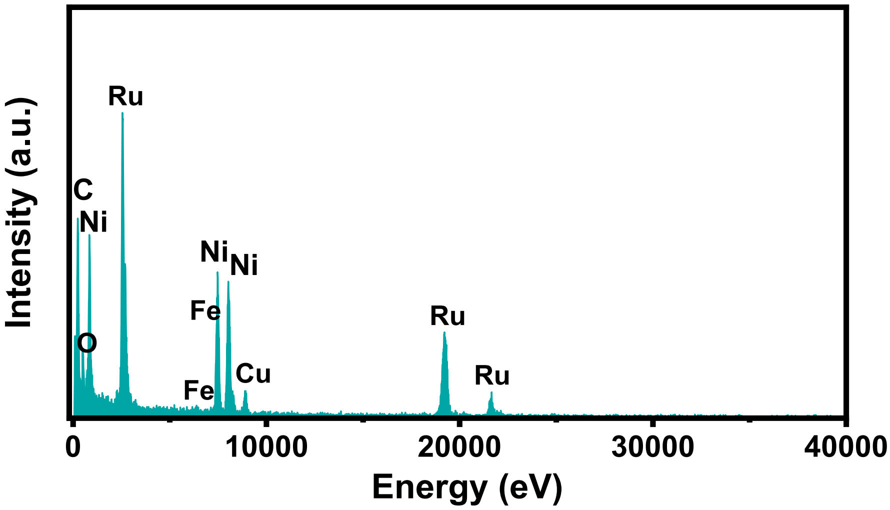

Fig. S3 The EDS spectrum of Fe_1Ru_2/NF.

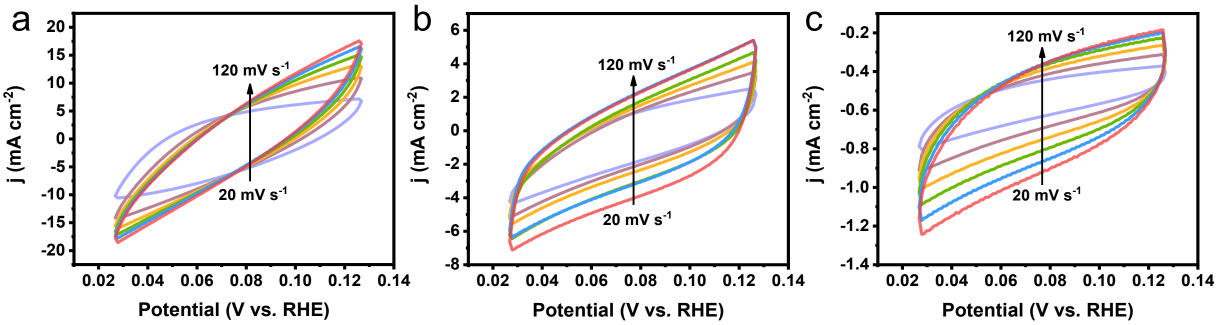

Fig. S4 CV curves measured in 1 M KOH at the scan rates from 20 to 120 mV s^{-1} for (a) Fe_1Ru_2/NF, (b) Ru/NF, and (c) Fe/NF, respectively.

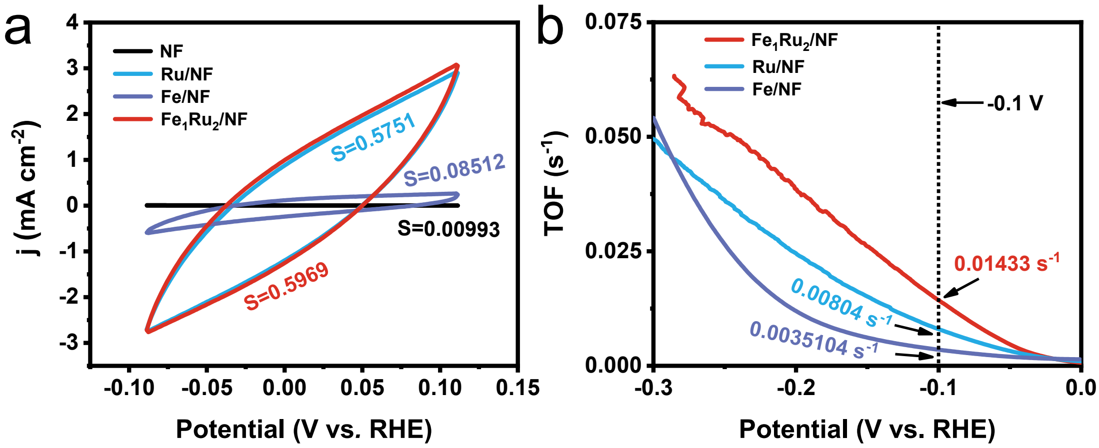

Fig. S5 (a) CVs of sample NF, Ru/NF, Fe/NF, and Fe$_1$Ru$_2$/NF for HER in PBS solution (pH =7) at a scan rate of 100 mV s^{-1}. (b) TOF values of samples.

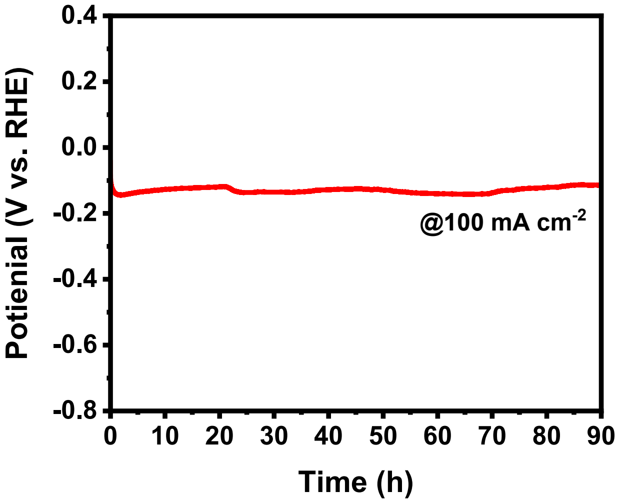

Fig. S6 Durability testing for the Fe_1Ru_2/NF electrocatalyst.

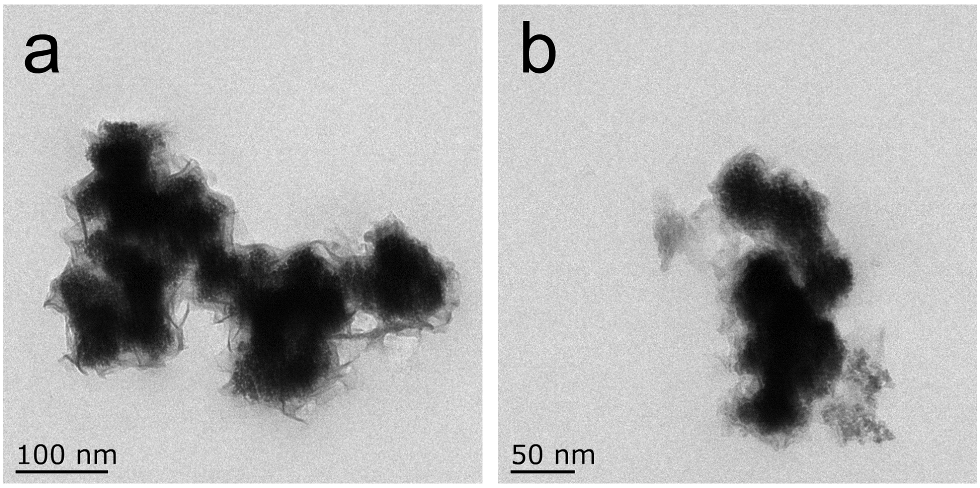

Fig. S7 (a, b) TEM images of Fe_1Ru_2/NF after stability test.

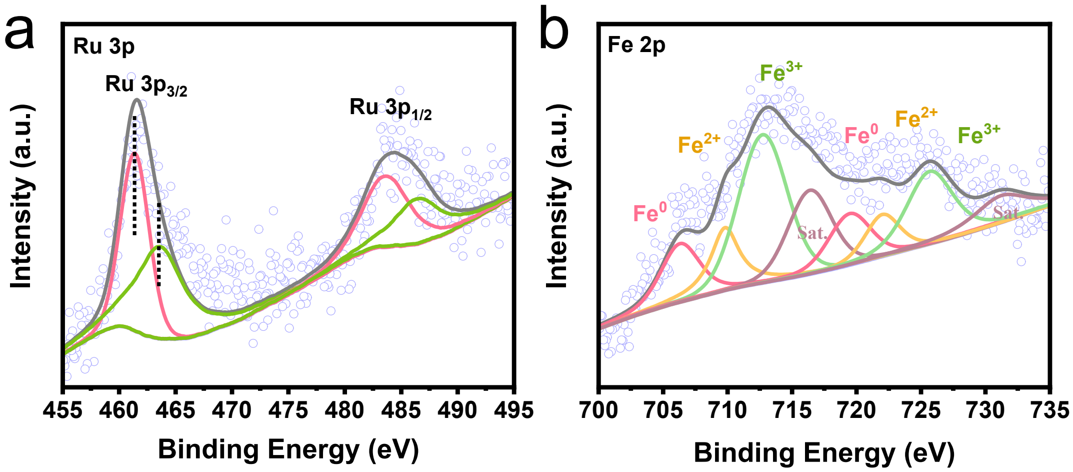

Fig. S8 High-resolution (a) Ru 3p XPS spectrum and (b) Fe 2p XPS spectrum of Fe_1Ru_2/NF after stability test.

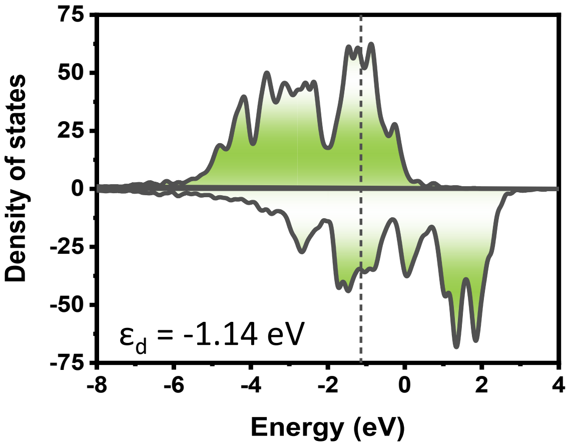

Fig. S9 The project DOS of Fe 5d orbit of Fe (ε_d = -1.14 eV).

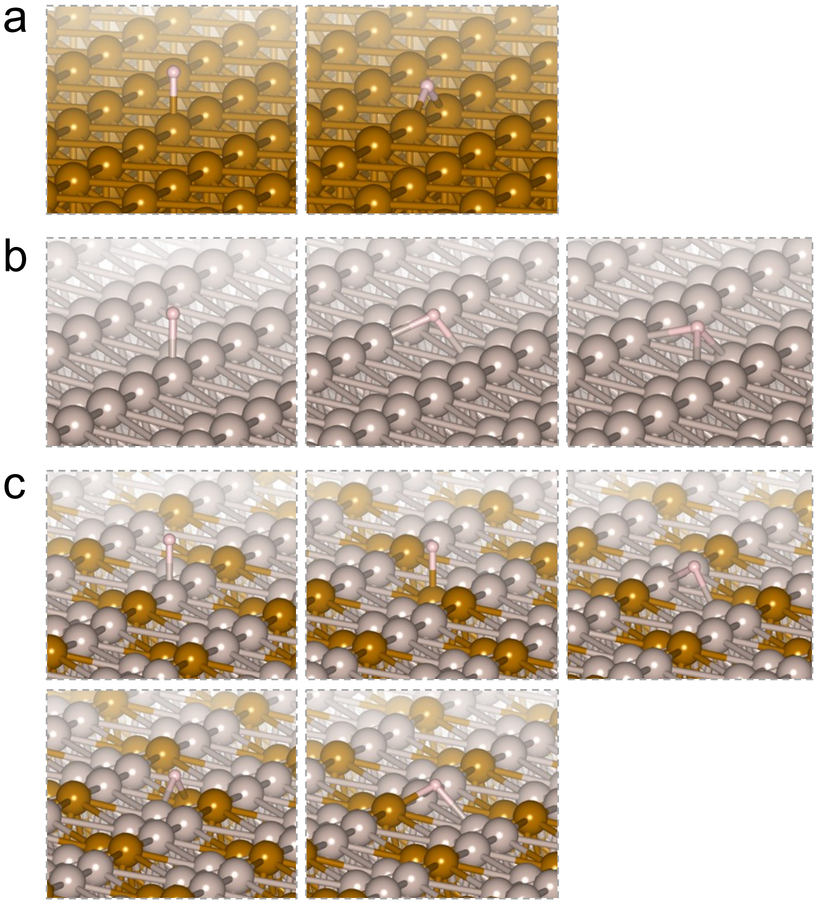

Fig. S10 H* adsorption configurations on (a) Fe, (b) Ru and (c) Fe_1Ru_2 alloy.

As shown in Fig. S10a, H* can be adsorbed on the top and bridge sites of Fe. The absorption energies (E_{ads}) were -1.04 eV and -1.48 eV, respectively. For Ru, H* can be adsorbed on the top, bridge, and hollow sites, with E_{ads} values of -0.36 eV, -0.54 eV, and -0.65 eV, respectively (Fig. S10b). Regarding the Fe_1Ru_2 alloy, five sites for H* adsorption were investigated, namely the top of Ru, the top of Fe, the bridge between two Ru atoms, the bridge between a Ru and an Fe atom, and the hollow site formed by Ru and Fe atoms (Fig. S10c). The E_{ads} of these sites were -0.19 eV, 1.25 eV, -0.87 eV, -0.78 eV, and -0.68 eV. Consequently, the bridge sites of Fe, the hollow sites of Ru, and the bridge between two Ru atoms of Fe_1Ru_2 alloy were selected as the final HER active sites.

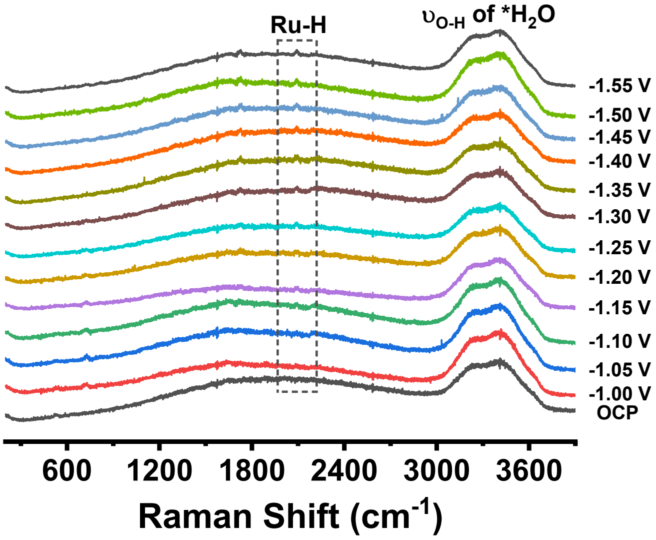

Fig. S11 In situ Raman spectra of Fe_1Ru_2/NF under various applied potentials in 1 M KOH solution.

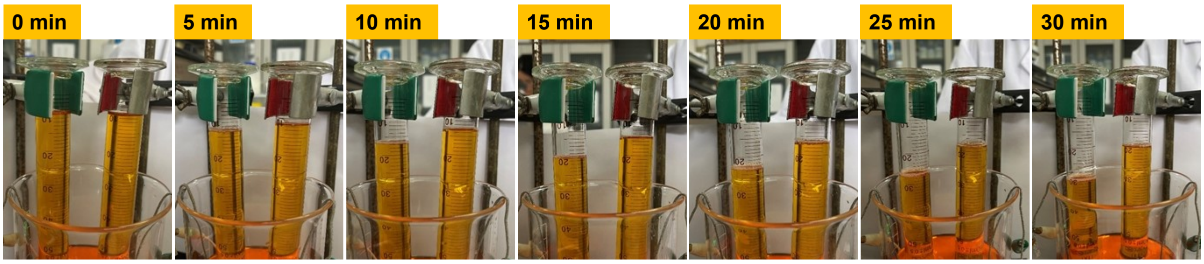

Fig. S12 The schematic diagrams for faradaic efficiency test using the water drainage method.